

## TOPICAL REVIEW

# Review and Analysis of Magnetic Energy Harvesters: A Case Study for Vehicular Applications

JAVAD ENAYATI<sup>1</sup> AND PEDRAM ASEF<sup>ID</sup> 1,2, (Senior Member, IEEE)

<sup>1</sup>School of Physics, Engineering and Computer Science, University of Hertfordshire, Hatfield, AL 109 AB, U.K.

<sup>2</sup>Department of Electronic and Electrical Engineering, University of Bath, Bath, BA 27 AY, U.K.

Corresponding author: Pedram Asef (p.asef@herts.ac.uk)

This work was supported in part by the European Commission under Grant KEEP/644.

**ABSTRACT** Energy harvesting (EH), as an enabling technology of energy derivation from ambient sources, has attracted much research attention in wireless sensor network (WSN) context. The magnetic energy harvester (MEH) introduces ambient energy harvesters' most promising technological development. This paper presents a review and analysis of MEH applications in WSN like vehicular systems and technologies. The successful approaches are introduced and classified based on technical characteristics and working principles. The fundamentals of their operation are discussed in detail, and the power points of each method are reviewed. To select the optimal energy harvester, in this work a case study is provided for feeding navigational sensors mounted on a rotating wheel of vehicles. Finally, the performance of the developed MEH model is evaluated and discussed for harvesting energy at the rotating wheels of a ground vehicle. To offer electromagnetic field analysis of the studied MEH, the simulations are performed in Ansys Maxwell software for further harvested power evaluation.

**INDEX TERMS** Magnetic energy harvester (MEH), wireless sensor network (WSN), energy management, electromagnetic simulation, vehicle technology.

## I. INTRODUCTION

With the emerging Internet of things (IoT), the technologies in wireless sensor networks (WSN) are developed to meet the main requirements of the data management systems [1], [2]. The main goal of the IoT platforms is the precise measurement of the operational condition of the underlying system. The gathered information can be used for different purposes such as real-time control, monitoring, maintenance scheduling, etc. WSN as the heart of the IoT systems plays a key role in the satisfactory operation of the entire system. WSNs have a wide application in health care monitoring, environmental sensing, industrial monitoring, as well as connected and autonomous vehicles [3]. Energy supply system (ESS) is one of the primary parts of the WSNs. ESS consists of a set of electromechanical devices for providing an uninterrupted feed to the sensor network. The rules governing the

energy supply mechanisms for efficient feeding of the sensor nodes are known as energy management systems (EMS). The main aim of the energy system in a WSN is high-quality energy provision for different parts of the network without any energy deficiencies [4], [5]. Nevertheless, conventional methods of energy systems have limitations in highly integrated field conditions where sensors are mounted in harsh environments [6]. In some situations, the energy provision system is the main bottleneck in the deployment of the WSNs [7]. The situation can be exacerbated particularly when it is difficult to find a suitable source of energy close to the sensor nodes [8], [9].

Energy harvesting (EH) techniques that mainly convert the environmental energy sources including solar, thermal, electromagnetic and vibrational energies into the electrical form for empowering electronic devices have been a wide area of scientific research over the past decade [10-], [11]. They are known as enabling technology providing energy to WSNs. Among EH methods, magnetic energy harvesters (MEHs)

The associate editor coordinating the review of this manuscript and approving it for publication was Zesong Fei<sup>ID</sup>.

have potential to implement high-performance energy converters for mostly small-scale consumers. For the sake of acceptable energy density, size flexibility, and simple structure, the MEHs have wide applications in instrumentation. For designing MEHs, the main complexities are related to the electrical circuit for implementing a power management system. The impedance matching, voltage control, and electronic elements are some of the considerable challenges to be addressed when a power management system is designed for MEHs [12]–[15]. The optimal design of the geometry of electromagnetic harvesters is also an attractive subject to enhance the efficacy of the system. For example, in [16], the researchers proposed a pick-up coil with a magnetic back iron to maximize the output voltage. Additionally, several pieces of research are dedicated to applying MEMS technology in the tiny energy harvesters in order to cope with the size limitations [17], [18]. Magnetic, vibrational, thermal, ambient light, and RF sources are the most popular initial types of energy that can be converted utilizing MEMS technologies [19]–[21].

To harvest electric energy from magnetic fields, different conversion forms exist. Electromagnetic induction is the most well-known method in this context. The process relies on generating voltage which applies variable magnetic flux around a coil to induce an electrical voltage in the coil. The achieved energy density obtained by this approach is relatively higher than the other competitors. The flowchart of the energy conversion process in a MEH system is demonstrated in Fig 1. As presented, environmental energies are applied to a magnetic variation system to induce electrical energy into the coil circuits based on Faraday's law of induction. Then, the converted energy is regulated by the EMS system. The regulated energy is used to feed the sensors or a storage system. Alternatively, the stored energy can be used to feed the sensors when the environmental energy is less than the convertible level.

Two types of induction-based electromagnetic conversion method exist. The stand-alone induction structure (type 1) harvesters operate independently, in which the harvesting coil embedded far from the variable magnetic flux [22]. The second type is the dependent coil structure, in which the coil is clamped on the section of the magnetic flux source. The MEH approach can also be categorized based on size requirements, insulation factors, packaging and installation conditions, safety measures, and required energy.

As the energy density of the MEH is noticeably higher than the other harvester types, the systematic investigation of the MEH in the context of the WSN is intensively required. A systematic review [23] based on mechanical energy harvesting methods is recently investigated. As reported, the knowledge of mechanical energy harvesting is taxonomized to highlight the advantages of these types of harvesters to be utilized in the industrial applications. This review paper focuses on the approaches of EH from magnetic fields. The main contributions of the paper are as follows:

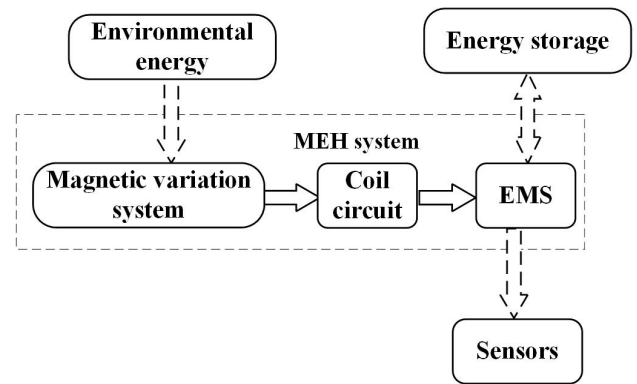


**FIGURE 1.** Flowchart of energy conversion process in a typical MEH system.

- 1) A detailed explanation of operation principles of recent MEH methods is presented.
- 2) The presented methods are taxonomized based on the design characteristics and the successful works are highlighted.
- 3) A comparison study in terms of electrical and mechanical properties for a delegate application in feeding the sensors of the rotational coordination is performed.
- 4) A set of 2D simulations in Ansys Maxwell software are performed to assess the applicability of the selected method.

## II. FUNDAMENTALS OF MEH

Based on Faraday's amp law [24], a variable voltage  $V$  is induced into the electric circuit when a variable magnetic field  $d\phi$  interacts with the circuit as given in:

$$V = -\frac{d\phi}{dt} \quad (1)$$

Variable magnetic fields can mainly be created by motion, either rotational or translational, and electrical switching circuits [25], [26]. The field strength is directly dependent to the material of the magnet and amplitude of the magnetic flux. Studies in [27]–[33] explored the effect of different parameters on magnetic field strength. Field strength and frequency of the variation alongside with the electrical topology of the harvester circuit (usually a coil) are determining factor in the level of the harvested power [34], [35]. MEH methods serve higher energy density compared to the other harvesting methods while keeping their insulation safety properties. The range of harvested energy is considerably large from a few micro-Watts to several Watts.

To achieve a detailed view of the final electrical parameters, the employed models are illustrated by analytical equations [36]–[38] or simulated by finite element (FEM) simulators [39]–[41]. However, the effect of magnetic material on the coil and geometric parameters are obtained more accurately by FEM analysis mainly when frequency analysis in a non-linear system is targeted [42]. Because of the unique characteristics of the magnetic waveforms, such as amplitude and frequency adjustment, the EMSs are flexibly developed

in the MEH systems. Hence, several pieces of research are conducted in this field [43]. The main goal of these works is to conduct maximum electrical power to the load in all operational frequencies and load impedances [44]. Nevertheless, commercially successful energy harvesters based on magnetic induction are still relatively limited. Considering the placement of the harvester (pickup coil) part relative to the variable magnetic field, the MEH approaches can be divided into two categories: dependent and independent. In this paper, the MEH methods are explored, and their operation principles are discussed based on these two main categories. Fig. 2 presents the overall classification of MEH methods.

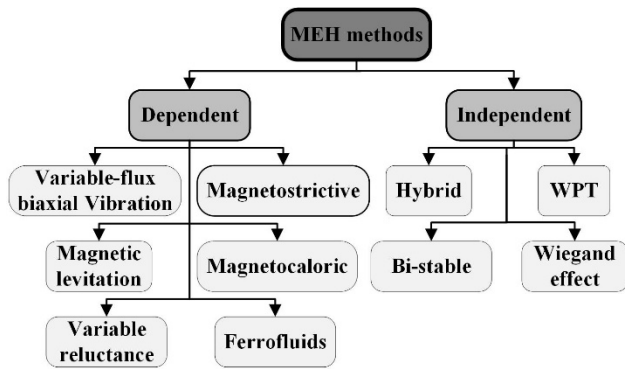


FIGURE 2. Classification of MEH methods.

III. INDEPENDENT MEH METHODS

The independent induction structure is a set of harvester coil and a magnetic field source away from each other. The main advantage of the independent induction structure is higher flexibility as there is no strict localization constraint. However, in most designs, the demagnetization factor and energy density are challenging issues [45]. This has been an inspiration for researchers to propose a harvester that captures the maximum energy when the core is placed in saturation [48]–[50]. Authors in [46] and [47] explored the advantages of independent MEH methods and proposed a novel harvester, in which the path of the magnetic flux is directed in a helical core leading to a lengthened flux path. In the following subsections, the successful independent MEH methods and their operational basics are discussed.

A. HYBRID

Hybrid MEHs include a variety of methods that combines different EH methods while the main function part relies on magnetic field properties. Most of these methods apply a combination of piezoelectric and electromagnetic harvesters that demonstrated improved output power on a small scale compared to other types of hybrid techniques [51]. They are mainly manufactured in a multimode structure intended for harvesting the highest power level from Kinetic energy sources for wideband operations. Principally, a piezoelectric harvester converts the mechanical strain of the active materials to electrical energy and the extracted energy is relative to

the strain amplitude of the structure [52], [53]. On the other hand, an electromagnetic harvester applies the relative motion between an electrical circuit and a magnetic flux to induce electricity into the circuit. The harvested energy is dependent on the relative speed of the moving part of the structure [54]. In the hybrid structure, the moving part contains permanent magnet (PM) objects and piezoelectric beams. A pickup coil is in the middle of the PMs. As the structure becomes active, the moving part vibrates, and both the piezoelectric beam and the pickup coil generate the electrical power. In such structures, the piezoelectric beam should be placed near a clamped edge, while the pickup coil is in the free end. The hybrid piezoelectric and electromagnetic harvesters in a simple structure are shown in Figure 3. Hybrid MEH methods are presented in recent research works repeatedly. Authors in [55] have reviewed the kinetic energy harvesters capturing the mechanical movement energy through magnetic transducers. Kinetic energy exists in the form of mechanical vibrations and displacements. A high-performance hybrid piezoelectric-electromagnetic energy harvester is also presented in [56], in which the output power can reach up to 80 mW.

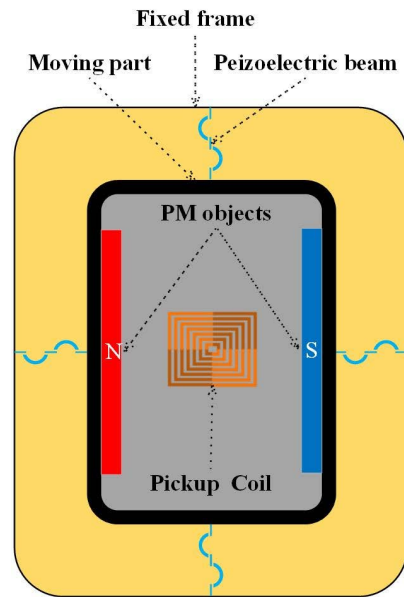


FIGURE 3. Hybrid piezoelectric and electromagnetic harvester topology.

B. WIRELESS POWER TRANSMITTER

The functionality of wireless power transmitters (WPTs) is the same as transformers and they work based on the law of magnetic induction. WPTs are usually applied as energy harvesters to scavenge the optimum energy from RF and other high-frequency magnetic fields [57], [58]. The high-frequency energy resources can be utilized in harsh environments where energy transfer is one of the main challenges for WSNs [59], [60]. Using WPT method, the sensor node can be extended with lower limitations. The high-frequency signals can be found everywhere in our environment. Therefore, many investigations are conducted to propose EH from

high-frequency fields. For instance, a harvester to collect the RF energy emitted by CFLs, and a rectifier are proposed in [61]. The ultra-high frequency WPT harvesters can work in the far-field. While their power range is low, they are used for applications with a long-range where the targeted nodes are far from the RF source.

In a high-frequency WPT, a switching circuit in the primary coil (transmitter), produces a variable magnetic field. The variable flux passes through the secondary coil (receiver) and induces an electrical voltage into the secondary coil. The induced power can be consumed by the dedicated load. Wireless chargers are also designed to harvest energy at relatively high levels. To guarantee the high rate of delivered power, the alignment of transmitter and receiver and their distance should be optimized [62], [63]. Fig. 4 indicates a simple topology of the WPT energy harvester. An overview of advances in WPTs as energy harvesters is provided in [64] and [65], the authors also presented several promising applications to depict future trends. Future power networks are prone to apply WPT energy harvesters as they have the potential for feeding low-power measuring devices in power systems [66]. Researchers in [67] presented a survey on the opportunities and challenges of utilizing WPTs in distributed WSNs to study the performance of these types of energy harvesters in IoT ecosystems.

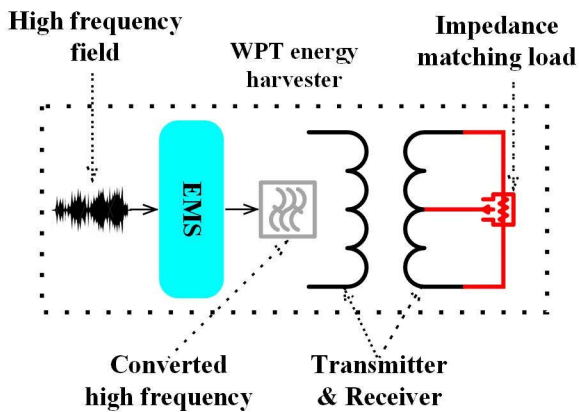


FIGURE 4. Working topology of a WPT energy harvester.

**C. BI-STABLE**

A bi-stable energy harvester can be designed magnet-freely [68]. Whereas typical bi-stable EH procedure has two magnets to create a double-well potential function. One magnet is fixed on a moving piezoelectric cantilever, and the other is mounted on a spring. The two magnets are placed opposite each other and fixed to a base. If an external excitation is exerted on the base, the cantilever beam starts vibration. When the magnet mounted on the cantilever moves toward the magnet on the opposite side, the repulsive force reaches its maximum value. Then, the spring is compressed and the distance between two magnets increases, this is known as the first stable state. As the cantilever-mounted magnet moves

away from this position, the repulsive force between the magnets decreases. Due to spring restoring force, the spring-mounted magnet returns to its initial state (second stable state). The operation of bi-stable MEH is shown in Figure 5. The bi-stable MEHs can operate in the low frequencies and solve one of the basic challenges in low-frequency broadband magnetic field, in which the capability of energy harvesting is low [69]. They also provide a solution to the challenge of scaling down harvesters to MEMS applications. Different existing designs of bi-stable energy harvesters are presented in the literature [70]. In [71], a MEH is developed to harvest the vibrational energy in wideband by incorporating the effects of both bi-stability and mechanical impact into a single device. The effect of adding a spring loading magnet in increasing the range of harvestable excitations is explored in [72]. The researchers proved that the cantilever would be able to overcome the magnetic repulsive force even in small excitations. To enhance the performance of the bi-stable harvester at low frequencies, the spring is replaced with bellows in [73] and the final structure demonstrates a satisfactory performance in 2 to 15 Hz excitation.

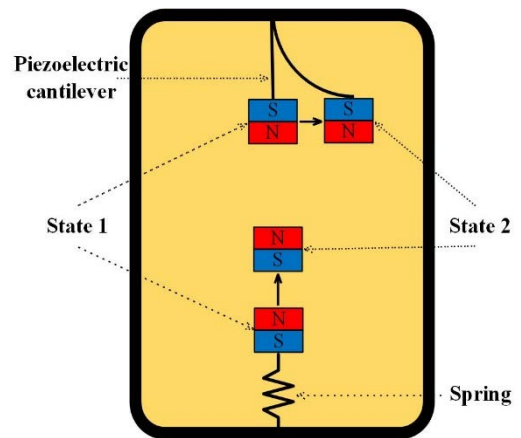


FIGURE 5. Bi-stable working topology of a WPT energy harvester.

**D. WIEGAND EFFECT**

Wiegand-effect harvester is a type of MEH that applies Wiegand’s wires to generate a pulsive voltage in the dedicated coil [74]. Wiegand wires contain a magnetic shell with high coercivity, while the core of the wires is made of materials with soft magnetic properties. In the presence of the time variable external magnetic field, the inner core magnet, which is shielded by the magnetism of the hard shell, is protected against the variation of the magnetic field until the field strength eventually overcomes the protection. Next, a sudden polarization change happens which leads to a large voltage pulse at the Wiegand wire. The voltage pulse has a triangular shape, and its amplitude reaches several volts. As the magnetic field increases, it neutralizes the magnetic domains of the shell. Both the shell and core produce the same magnetization polarity where a second voltage pulse with lower amplitude is generated. The Wiegand-effect magnetization



curve has a trapezoidal shape. The operation principles of the Wiegand MEH, the related magnetization curve, and induced voltage in the Wiegand wire are demonstrated in Fig. 6.

The high-speed switching of magnetic polarization in the Wiegand wire generates a significant voltage which makes it valuable for higher voltage energy harvesters. The generated voltage can be easily converted to the target level in high voltage applications. It should be mentioned that the amplitude of voltage pulses does not depend on the variable magnetic field frequency. This property makes the Wiegand harvesters an attractive option for low-frequency energy harvester designs [75], [76]. In [77], a Wiegand-effect harvester is developed that can extract the energy from the changes in magnetic polarities in a magnetic positioning measurement system. In another study [78], a Wiegand-effect harvester applying an eccentric swinging pendulum is investigated. In this study, Wiegand wires are mounted on a wheel and convert the kinetic energy into electrical energy to supply the measurement equipment mounted on the wheel.

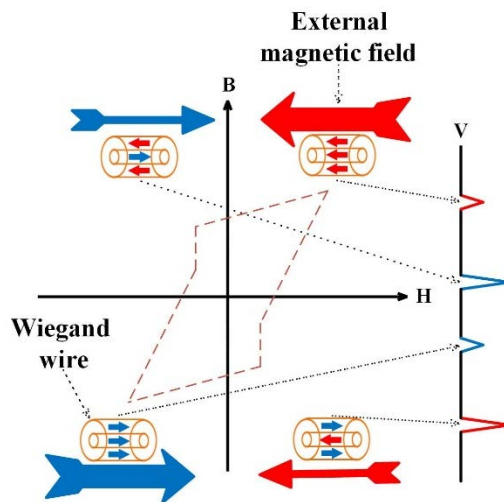


FIGURE 6. Wiegand MEH, operation principles, magnetization curve, and induced voltage.

#### IV. DEPENDENT MEH METHODS

Because of the great flexibility and high magnetic field intensity, the dependent induction methods in which the harvesting coil clamps the section of the variable magnetic flux source, has attracted much attention. Detailed studies have been conducted in this area of research to superimpose the strayed fluxes for achieving more concentrated flux linkage [79]. In several investigations, the dependent coil design is developed to harvest the maximum energy from low-frequency magnetic field variation. These low frequencies of energy can be found in many practical applications [80]–[84]. Examples of such techniques are applied to generate electrical energy from the body motion of the human [85], [86]. In some cases, the dependent coil is attached to the source of the magnetic field to minimize the air gap. Based on the reported results, the harvesters can be successfully used for WSNs

to achieve continuous power measurements. The dependent MEH methods are explored in the following subsections.

#### A. VARIABLE-FLUX VIBRATION

Variable-flux vibration (VFF) energy harvester is a novel type of MEH, in which a ferromagnetic object is moved into the magnetic flux path of the fixed PMs. Leading to disruption of the magnetic fields of the PMs. As a result, an electrical voltage is induced across a pickup coil which is mounted in the nearby field. The basic structure of a VFF is shown in Fig. 7. The structural mechanism has the advantage of applying a stationary magnetic circuit and coil that prevent the interactions. Also, the mechanical complexity and output power density are optimized in the VBHs. The authors, in [87], proposed a variable-flux bi-axial vibration energy harvester for low-frequency and low amplitude vibrations applications. The experiments showed efficient performance of the system at a mean frequency equal to 6.5Hz. A bandwidth of 5.8 Hz is provided for the harvester, whilst its maximum output power reached  $154\mu\text{W}$ .

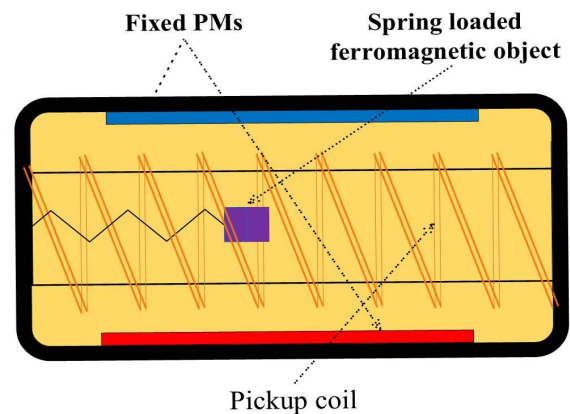


FIGURE 7. The Basic structure of a VFF energy harvester.

#### B. MAGNETOSTRICTIVE

The principle of operation in magnetostrictive harvesters is based on two main steps. Firstly, mechanical energy is applied to magnetostrictive materials. The mechanical energy is converted to magnetic energy using magneto-mechanical coupling. This is also known as the Villari effect (magneto-mechanical effect). According to the Villari effect, the magnetization domain of magnetostrictive material is changed, when mechanical stress is applied. In the second phase, the magnetic energy is converted to electrical energy in an electrical circuit (pick-up coil) based on Faraday's law of induction. Also, a static magnetic domain using a PM is utilized, as domain initial bias. Samples of magnetostrictive materials are explored in [88]. Magnetostrictive materials can play a key role in the development of EHs. For the sake of their high-specific energy, there is scientific research on them to extend their application for the industrial purposes [89]. Since considering the general behaviors of magnetostrictive

materials cannot be directly captured, a FEM analysis is conducted in [90] to cover fully coupled nonlinear modeling of the magnetostrictive materials. Authors in [91] and [92] explored the properties of harvesters based on a magnetostrictive amorphous core. They proved that these materials are applicable for scavenging low-energy vibrations when they are directly subjected to axial movements. Fig. 8 illustrates the basic operation of the magnetostrictive MEH. The magnetic flux density of magnetostrictive materials is calculated by:

$$B = d \cdot \varepsilon + \mu^\varepsilon \cdot H \quad (2)$$

where  $B$  is the magnetic flux density.  $d$  and  $\varepsilon$  are magnetostrictive constant and applied stress to the magnetostrictive material, respectively. The permeability of the flux path depends on the stress value, and thus, it is shown by  $\mu^\varepsilon$ . The parameter  $H$  is the magnetic field strength.

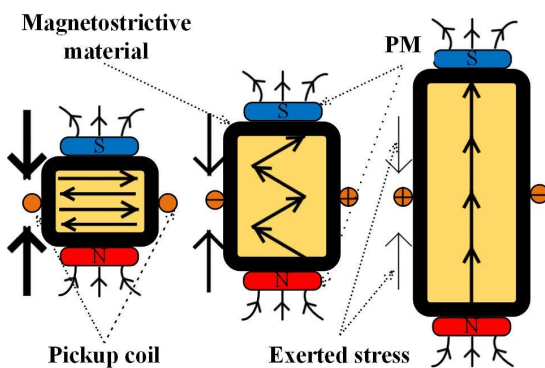


FIGURE 8. Basic operation of the magnetostrictive MEH.

### C. MAGNETIC LEVITATION

The Magnetic levitation (maglev) harvesters mostly work based on the levitation phenomenon. They typically consist of a nonmagnetic container with two PMs installed on both end extremities of the container. A third PM is levitated in the container between the fixed PMs [93]. The levitation force comes from the arranged polarity of the PMs such that the same magnetic polarity repels each other with the force  $F$  as:

$$F = \frac{B^2 A}{2\mu_0} \quad (3)$$

where,  $B$  magnetic flux density,  $A$  is cross sectional area, and  $\mu_0$  is space permeability. Also, a pickup coil is wound around the outer surface of the container to harvest the kinetic energy of the levitated magnet in form of electrical energy [94], [95]. A typical maglev system is demonstrated in Fig. 9. Several pieces of research studied magnetic levitation, in which a dependent coil is utilized to harvest the energy of the levitated magnet [96]. In [97], the authors proposed a maglev unit to convert ambient vibration with stochastic directions into a unique motion direction of a central levitated magnet. As a result, the frequency bandwidth is increased. Researchers [98] have used a three-layer magnetostrictive

material (Terfenol-D/PZT/Terfenol-D) as a levitating magnet. The complex has a high energy density which leads to generating high power at low-frequency bounds. The use of magnetic levitation eliminates the need for a mechanical spring and increases the energy density of the complex. In [99] and [100], the authors proposed an energy harvester based on the magnetic levitation springless structure and a mechanism with velocity amplification. As a result of the high achieved acceleration, more vibration energy can be harvested. It is shown that such topology is appropriate for loads with high peak power. Magnetic levitation-based MEHs are also known as track-born energy transducers that can be applied for harvesting the vibration energy of railways. They are the best electrical supply source for feeding the wireless sensor node in remote railways. Studies in [101] and [102] have focused on maglev MEHs which aim to scavenge vibration energy in railways for instrumentation purposes. The results presented that these kinds of harvesters can satisfy the environmental conditions and sensor supply requirements for the railways.

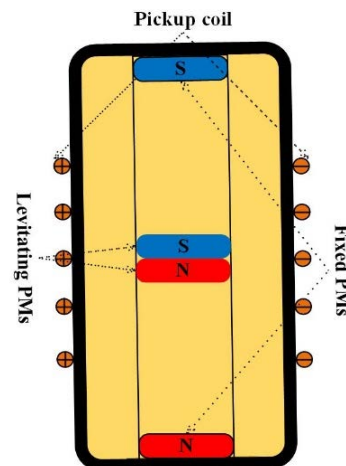


FIGURE 9. Typical maglev system.

### D. MAGNETOCALORIC

The magnetocaloric effect has been discovered about two decades ago. Nowadays, there are unprecedented choices between numerous magnetocaloric materials (MCMs). The LaFeSi is a well-known and widely applied MCM for designing the energy harvesters [103], [104]. Also, Gadolinium films in a thickness range between a few to tens of microns are another option for MCMs in the EH applications [105]. As the main properties, MCMs heat up, when brought into a magnetic field. In the energy harvesting process, the MCM is usually suspended on a cantilever beam which is located between a hot source and a heat sink. The MCM loses its magnetization in the hot location and reaches its peak magnetization in a cold location. An outer magnetic field like a PM which is mounted on a heat source triggers the MCM to oscillate between hot and cold sources. Fig. 10 demonstrates the working principles of the magnetocaloric energy harvesters. Researchers in [106] explored the optimal size

of the cantilever which leads to the self-oscillation of the MCM between heat and cold sources. The kinetic energy corresponding to the oscillation is converted into the electricity using piezoelectric elements. The performance of the magnetocaloric energy harvesters directly depends on temperature gradients. In [107], a scientific model based on empirical relationships is developed to analyze the thermomagnetic properties of MCMs. The study investigated the energy density of magnetocaloric-based MEHs which is usually low, and they successfully generated electrical power for a range of micro-electrical system.

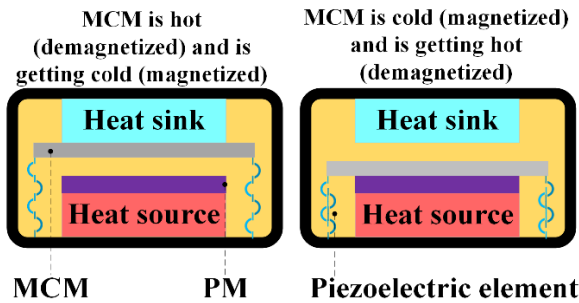


FIGURE 10. Principles of a magnetocaloric energy harvester.

E. VARIABLE RELUCTANCE

Common structure of a variable reluctance energy harvesting system (VREH) is composed of a toothed wheel and a PM. A pole-piece is also applied to complete the flux path. Both PM and pole-piece are made of ferromagnetic materials. A pickup coil is wound around the pole piece to harvest electrical energy. The reluctance of magnetic path  $R$  is changed to generate the variable magnetic field. Then, a proportional voltage  $V$  is induced into the pickup coil as in:

$$V \propto \frac{dR}{dt} \tag{4}$$

Fig. 11 depicts the schematic of the energy harvester using the variable reluctance (VR) principle. VREHs are industrially applicable types of power converters. They usually convert the commonly found rotary kinetic motion in a magnetic field. A vast area of research is focused on the implementation of VREHs to optimize the output power [108], [109]. In [110], the authors proposed and embedded VREH to power an integrated WSN in the railways. Surprisingly, the output power has reached around 80mW, which makes it suitable for feeding a wide range of wireless sensors including, speed, vibration, strain, and temperature measurement devices. In reference [111], the researchers have revealed that the three-phase topology enhances the VREH power performance compared to three single units. Additionally, the optimized arrangement decreases the torque ripple significantly when the rotation speed is relatively low. The authors in [112] investigated the VREH design using a m-shaped pole-piece. The final product achieved a compact structure with high power density, which makes it applicable for embedded and size-constrained cases.

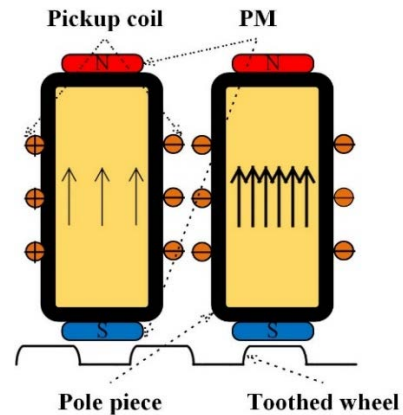


FIGURE 11. Principles of a magnetocaloric energy harvester.

F. FERROFLUIDS

Ferrofluids are some sort of liquids composed of nano-scale PM dipoles. While no external magnetic flux is presented, the magnetic dipoles are stochastically oriented. When an external magnetic field, from a PM, is exerted on the fluid, the dipoles are aligned parallel to the external field. This produces a net magnetic density in the fluid as:

$$B = \mu_0(H + M) \tag{5}$$

where,  $\mu_0$  is space permeability,  $M$  is ferrofluid magnetization which is proportional to magnetic field strength  $H$  by magnetic susceptibility  $X$  as in:

$$M = XH \tag{6}$$

A tube carrying the magnetized fluid can be put into a vibrational frame, in which its vibrations match the natural frequencies of the fluids. Considerable magnitude waves can be achieved on the surface of the fluid. The produced waves actively change the direction of the magnetic dipoles and create a variable magnetic flux. A pickup coil wound around the tube can harvest electrical energy in the variable magnetic field. The touching mechanism is eliminated in ferrofluids leading to lower friction in the harvester structure. This leads to efficiency improvement, which is the main challenge, in designing the energy harvesters. Fig. 12 presents the operation of the ferrofluid MEHs. Most studies in the MEH literature proposed the ferrofluids as dependent induction harvesters [113], [114]. For example, in [115], a ferrofluid based MEH is investigated to scavenge the human motion kinetic energy. The resonant frequency between 8 to 10 Hz is obtained which is higher than the normal activity frequency bound. However, it is suitable for energy harvesting in sports activities. To increase the operating frequency range to include the normal activity frequencies, the authors in [116], proposed a MEH composed of a combination of spring and ferrofluid. Parametric studies and performance analysis in [117] have revealed that the distance between the magnets and the ferrofluid surface, location of the magnets, and ferrofluid susceptibility are the most effective parameters on the

designed harvester performance. A non-resonant, Ferrofluid-based MEH is developed and reported in [118] to scavenge the kinetic energy over a broad frequency range. For this purpose, magnet arrays are suspended by the liquid bearing and mounted on a multi-layer coil plate such that the obtained MEH can output appropriate power for a wide frequency range.

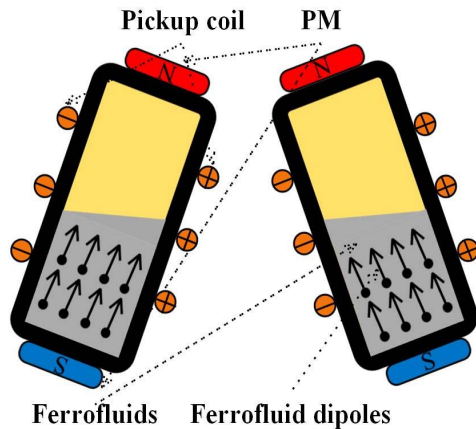


FIGURE 12. Operation of the ferrofluid based MEH.

### V. CASE STUDY: MEH DESIGN FOR ROTATING WHEEL OF PASSENGER VEHICLE

Selecting the best MEH for a delegate low-power application has always been a challenging process because several criteria should be considered to select the optimized harvester. In this paper, an investigation is carried out to select the optimal energy harvester which can feed navigational sensors and data transmission system mounted on a rotating wheel of a vehicle. Similar works in [78] and [119], are done to scavenge the kinetic energy of a rotating part. However, small-scale power is harvested in these works to feed a low number of sensors with low power consumption. In this work, a comparison study between different options is offered, in the previous sections, to evaluate the performance of the techniques to choose the optimum method. Then, the capability of the selected method is validated by applying electromagnetic simulations, using a 2D model, conducted in the Ansys Maxwell software.

Designing the whole system to have a comprehensive assessment of the system’s goals, where a fair comparison can be provided. Providing sufficient power, as the main target, to the load in a safe voltage range is desired. In this case study, the selected MEH should feed a combination of sensor and data transmission systems which are mounted on a rotating wheel. Corresponding power consumptions and the required voltage for the load elements are demonstrated in Table 1.

As presented in Table 1, the required voltage is in the range of 1.1-5.5V. In the standby condition, the accelerometer and RTC are active, where the power consumption is low. As the system is in data-gathering mode, the processor, IMU, and temperature sensors are electrically fed. The maximum power consumption occurs in data transmission mode when both

TABLE 1. Load elements and corresponding consumptions.

Load elements	Max power (mW)	Voltage (V)
Processor	13	1.8-3.8
Accelerometer	0.07	1.7-3.6
RTC	0.055	1.1-5.5
IMU sensor	15	2.2-3.8
Temperature sensor	6	2.5-5
Data transmission system	27	1.8-3.6

processor and data transmission system are active, and the consumed electrical power reaches around 40mW.

On the other hand, field strength and frequency of the variation are the determining factors in the amount of power generated by the applied MEH. The size issue is another parameter to be considered as installation and working conditions are limiting factors affecting the size of the dedicated MEH. Table 2 summarizes the notable studies carried out in the references of the paper. The MEHs are categorized based on the types and their important operational parameters are reported in the table. This table gives the initial idea for selecting the optimal type of the MEH.

Given the nature of the rotating system application, the best way to harvest the electrical energy is to scavenge the kinetic energy of the rotating part [78]. The operation frequency of the magnetostrictive materials is beyond the frequency band of the rotating wheels. The complexity of applying magnetostrictive materials in the EH system is another inhibitory factor for proposing this method [57]. Despite acceptable operation frequency range for the magnetocaloric and ferrofluids, the difficulties for utilizing the special and expensive materials still exist for these methods. Likewise, level of harvested power using these methods is limited [40].

The hybrid methods are usually employed for delegate and low space applications [65]. The power density of this method is relatively low and it requires many detailed specifications in the design phase. However, the magnetic levitation scheme unlike the bi-stable method meets the technical parameters of the specified load (power demand, operation voltage and frequency, and power density) and can be a suitable option if design complexities are neglected.

The Wiegand effect and VFV approaches not only have energy level issues [24], [114], but they also have unsuited voltage levels for the dedicated load. Despite their suitable frequency range, they cannot be considered a proper choice for the intended case study. A contradictory condition exists for the WPT-based MEH. Although this method has a high potential to achieve high power ratings [53], the operational frequency range is by far beyond the common rotating wheel frequency.

The frequency band of the variable reluctance scheme thoroughly meets the rotary frequency of the vehicle’s wheel. This method also has the closest voltage range of the load components. Moreover, the power range lies between several milli-Watts to a few hundred milli-Watts. Also, the power generating capability of this method theoretically suffices the load demands. The elements of a variable reluctance



TABLE 2. Operational parameters of the Studied MEH Technologies.

Type	Output voltage range (V)	Max output power (W)	Input frequency range (Hz)	Load ( $\Omega$ )	Acceleration (g)	Energy density	Flux density (T)
Hybrid* [3, 15, 65, 97]	0.27-0.8	640e-9	7-294			0.049-42.7 nW/mm <sup>3</sup>	
		80.1e-3	14	1e3-10e3	2		
		24.56e-6	10-20		1		
WPT* [53, 63, 81]	20	37e-3	2	10		0.3-1.9 mW/cm <sup>3</sup>	0.5
		20	1e5	20		4.22 mW/cm <sup>3</sup>	
		3.4e-3	1e8-24.5e8				
Bi-stable* [45, 54, 70, 78, 111]	1.377	2.1e-3	20-260e3	1e6-6e6		0.01-0.036 mW/cm <sup>3</sup>	
		179e-6	6.4-11.5	47e3			
		385e-6	1-95			0.43-0.52 $\mu$ W/mm <sup>3</sup>	
Wiegand effect* [113, 114]		19.3e-6	3.4-8	1e3	0.4-1.5	1.45 $\mu$ W/cm <sup>3</sup>	
		450e-9	1-90	300e3			
			2-15	5e3-1e8		0.02-4.49m W/m <sup>3</sup>	
VFV** [24]	0.85-1.4	1.15e-3	4-11	340			0.06-0.22
	1.5-3	1.5e-6	1-50	70-1.2e3			
Magnetostrictive** [56, 67]	0.0011-0.0012	154e-6	0.7-12.3	5.6-9e3		0.014-0.77 W/m <sup>3</sup>	
		18e-6	300	50		3 $\mu$ W/cm <sup>3</sup>	0.15
			100	10		20 $\mu$ W/cm <sup>3</sup>	0.5
Magnetic levitation** [7, 8, 41, 49, 50, 119, 120]	2.32	119e-3	3-7	45			
	43.4			290		8 kW/m3	
	68.2	514e-6	9.7-11.6	4.8e6	0.8		
	105	1.1e-3	10	1e7	1	3460 W/m <sup>3</sup>	
	2.93-3.13	10.2e-3	8-13.5	250			0.0014
	1.8-3.6	5e-3	105-20.5		0.6		
Magnetocaloric** [74, 115]	1.5-4.5	17e-3	5-50		2		
	1-7	12e-6	0.12			6.8 $\mu$ W/cm <sup>3</sup>	
Variable reluctance** [18, 83, 121, 122]	3-15	4.2e-6	0.23-0.41			240 $\mu$ W/cm <sup>3</sup>	
	2	840e-6	15			157.66 nW/mm <sup>3</sup>	0.25
Ferrofluids** [27, 40, 99]	1.2-4.2	76e-3	120-360	38.9-69			
		2.12e-3	8-16				
	0.005-0.2	220e-6	7.5-90			2.7-5.1 W/cm <sup>3</sup>	0.7
	0.0035-0.018	1e-6	6-14	35	0.25-0.3		
		9.5e-3	8-10	2.5	80.5		
	0.061-0.094	27.5e-6	2-4	80	2	10.5.25 W/cm <sup>3</sup>	

Note that \* indicates the technologies with independent MEH type, and \*\* shows the dependent MEH techniques

EH systems are off-the-shelf items. This method has the least implementation complexity among all reviewed techniques as it has a simple structure. Because of the mentioned advantages, the variable reluctance MEH is proposed for the conducted case study. The following subsections illustrate the simulation and results of the studied method.

**A. VARIABLE RELUCTANCE MEH SIMULATION USING FINITE ELEMENT ANALYSIS**

A variable reluctance for a prototype vehicle is simulated in 2D using Ansys Maxwell software. A PM with high magnetic permeability  $\mu$  is applied to provide the required magnetic field in the space. The commonly used NdFe35 is selected as the core material for the two PMs. The PMs are mounted on a fixed frame in the front suspension of the vehicle. This allows minimizing the distance between PMs and the rotating wheel to maximize the magnetic field strength in the pickup coil which has an iron core. Since the air gap in the flux path is relatively high, the saturation and core loss are negligible. The number of turns in the pickup coil is proportional to the generated voltage. Nevertheless, a high number of turns increases the coil resistance which results in power loss in the coil. In this case, the resistance of the coil winding is

around 0.85 $\Omega$ . As compared to load impedance (300 $\Omega$ ), the coil copper loss is very low. The pickup coil is fixed to the rotating wheel using a bracket such that it sweeps the PMs' flux in each rotation. Then, it can harvest the kinetic energy of the wheel. The harvested energy is transferred to the load components which is rotating with the coil synchronously. The diameter of the wheel is selected 700mm. Based on vehicle speed, the corresponding angular rate can be calculated. This is a conceptual design that is to be validated using the finite element analysis (FEA) simulation. The schematic of the designed variable reluctance MEH and the design parameters are described in Fig. 13 and Table 3, respectively. The simulation results are reported and discussed in the following subsection.

**B. SIMULATION RESULTS**

Different sets of electromagnetic 2D simulations are performed in Ansys Maxwell software to show the performance of the utilized technique in harvesting the energy of a rotating wheel. Simulations are conducted in a wide range of effective parameters to verify the adequacy of the designed system. The following subsections discuss the details of the simulations.

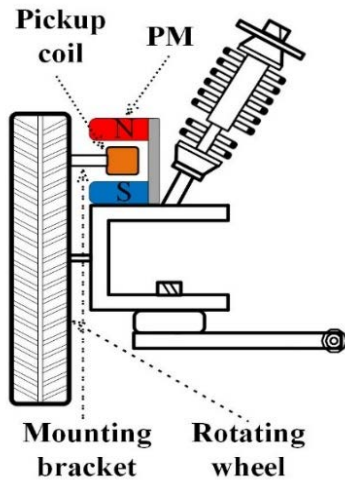


FIGURE 13. Schematic of the designed variable reluctance MEH.

TABLE 3. Design parameters of the variable reluctance MEH.

Nominal vehicle speed (m/s)	Nominal angular velocity of coil (rad/s)	Nominal air gap (mm)	PMs' size (mm×mm×mm)
22	$20 \times \pi$	50	70×20×20
Coil size (mm×mm×mm)	No. of winding turn on the coil	Coil resistance ( $\Omega$ )	Load impedance ( $\Omega$ )
60×20×20	150	0.85	300

1) SIMULATION WITH STANDARD DESIGN PARAMETERS

For the first case, a simulation with standard design parameters reported in Table 3 is performed. The side view of the simulated PMs, pickup coil, and rotation path (in terms of the field intensity and magnetic flux) is presented in Fig. 14(a-c). When the pickup coil enters the air gap between the PMs, the reluctance of the flux path decreases suddenly and pulsive power is harvested. The instantaneous voltage waveform is demonstrated in Fig. 15. The maximum and mean harvested powers are 4.17W and 251mW for this case.

2) SIMULATION WITH VARIABLE VEHICLE SPEED

A set of simulations is run to explore the effect of vehicle speed on the harvested power. For this purpose, the vehicle speed and proportional angular velocity of the coil are changed in each simulation. Other parameters are kept constant as given in Table 3. Fig. 16 demonstrates the obtained instantaneous voltage of different simulations corresponding to the vehicle speed. The more compressed the graph per unit time (higher vehicle speed), the higher the peak voltage is generated. This leads to higher harvested power and its growth rate. The maximum and mean harvested power respective to vehicle speed are shown in Fig. 17. As previously mentioned, the required average power is 40mW. However, when the vehicle speed decreases below 8.7m/s, the harvested power does not suffice the load requirements. Therefore, EMS is required to charge and discharge the ESS for effectively delivering continuous power to the load, regardless of the vehicle speed (e.g. below 8.7m/s).

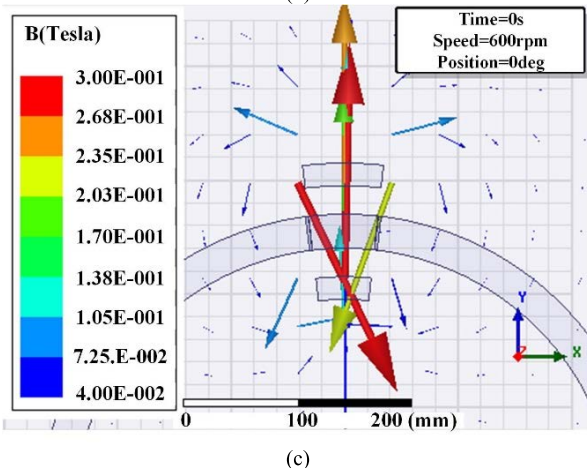
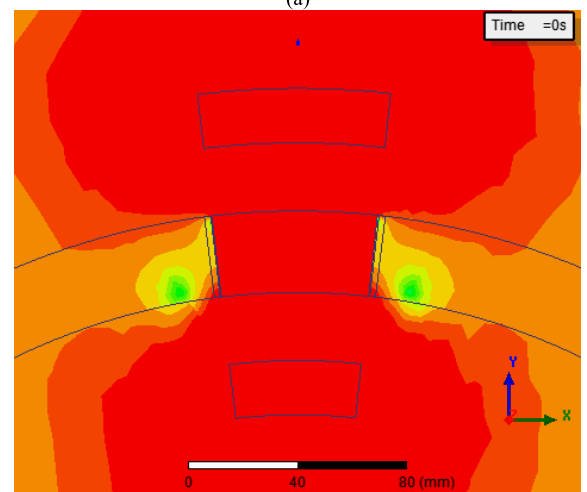
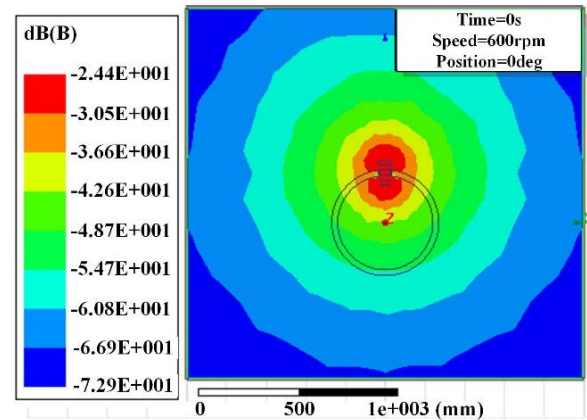


FIGURE 14. Side view of 2D mode for FEM simulation showing (a) the field intensity, (b) zoomed PMs, and (C) magnetic flux orientation.

3) VARIABLE AIR GAP ASSESSMENT USING FEM SIMULATION

Because of the unwanted vibrations in the rotating wheel, application of variable reluctance harvester has mounting complexity. In practice, the air gap between PMs and pickup coil is affected by the vibrations leading to variation in the harvested power. Hence, results of several simulations considering air gap variations are discussed in this section.

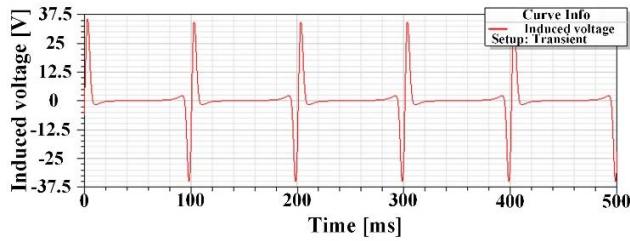


FIGURE 15. Instant voltage obtained from FEM simulation using MEH standard parameters.

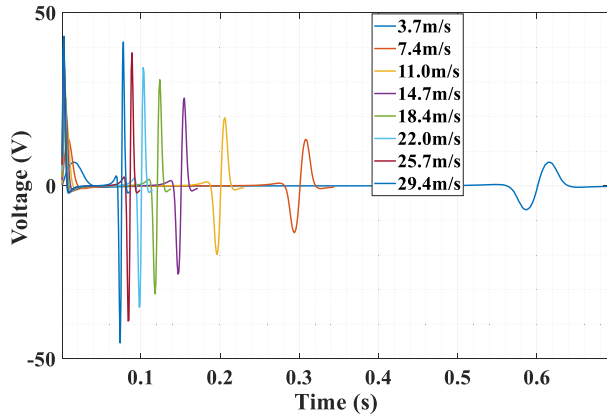


FIGURE 16. Changes of instantaneous voltage respective to the variable speed.

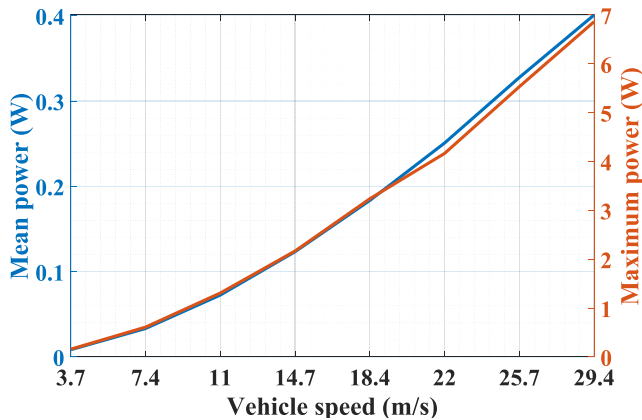


FIGURE 17. Changes of maximum and mean power respective to the variable speed.

The gap variation is selected considering the typical vibrations in passenger vehicles. The air gap between PMs and pickup coil is changed in each simulation, while other parameters in Table 3 are kept unchanged. Undoubtedly, higher electrical voltages induced in the pickup coil in lower air gaps. The voltage waveforms are varied as a function of airgap length, the produced different voltages are shown in Fig. 18. The maximum and mean harvested power corresponding to simulated air gaps are reported in Fig. 19. As presented, decreasing the air gap results in enhancing harvested power and its growth rate. Hence, the harvested power does not satisfy the load requirements in transmission mode if the air gap exceeds 119mm.

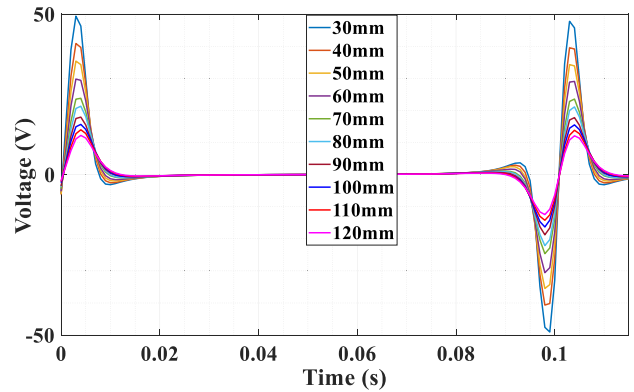


FIGURE 18. Changes of instantaneous voltage respective to the variable air gap.

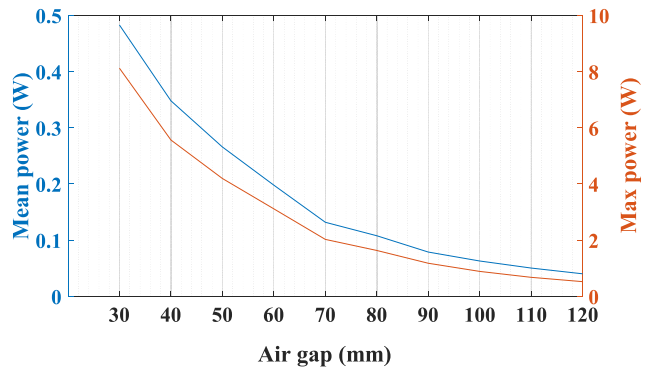


FIGURE 19. Changes of maximum and mean power respective to the variable air gap.

## VI. CONCLUSION

This paper presents a comprehensive review and analysis of applied MEH techniques. In two main categories, such as dependent and independent for utilizing in WSNs. The technical characteristics and working principles of each method are explored in detail. Additionally, the functional properties of electrical parameters are discussed to give a better view of the effective classification of the presented methods. Based on the comparative overview offered, an optimal energy harvester for feeding navigational sensors mounted on a rotating wheel of a passenger vehicle is proposed. An EH system based on a selected harvester type is simulated using 2D FEA in the Ansys Maxwell environment. The results of the electromagnetic field and electrical outputs are evaluated to demonstrate the suitability of the desired method in dedicated applications. Finally, an optimal variable airgap assessment has determined the optimum airgap in this work.

## REFERENCES

- [1] G. Dileep, "A survey on smart grid technologies and applications," *Renew. Energy*, vol. 146, pp. 2589–2625, Feb. 2020.
- [2] F. Li, W. Qiao, H. Sun, H. Wan, J. Wang, Y. Xia, Z. Xu, and P. Zhang, "Smart transmission grid: Vision and framework," *IEEE Trans. Smart Grid*, vol. 1, no. 2, pp. 168–177, Sep. 2010.
- [3] G. M. Karageorgos, C. Manopoulos, A. Kiourti, A. Karagiannis, S. Tsangaris, and K. S. Nikita, "An approach for self-powered cardiovascular monitoring based on electromagnetic induction," *IEEE Sensors J.*, vol. 18, no. 1, pp. 83–93, Jan. 2018.

- [4] T. J. Kazmierski, G. V. Merrett, L. Wang, B. M. Al-Hashimi, A. S. Weddell, and I. N. Ayala-Garcia, "Modeling of wireless sensor nodes powered by tunable energy harvesters: HDL-based approach," *IEEE Sensors J.*, vol. 12, no. 8, pp. 2680–2689, Aug. 2012.
- [5] W. He, P. Li, Y. Wen, J. Zhang, A. Yang, and C. Lu, "A noncontact magnetolectric generator for energy harvesting from power lines," *IEEE Trans. Magn.*, vol. 50, no. 11, pp. 1–4, Nov. 2014.
- [6] A. Abasian, A. Tabesh, A. Z. Nezhad, and N. Rezaei-Hosseiniabadi, "Design optimization of an energy harvesting platform for self-powered wireless devices in monitoring of AC power lines," *IEEE Trans. Power Electron.*, vol. 33, no. 12, pp. 10308–10316, Dec. 2018.
- [7] J. Han, J. Hu, Y. Yang, Z. Wang, S. X. Wang, and J. He, "A nonintrusive power supply design for self-powered sensor networks in the smart grid by scavenging energy from AC power line," *IEEE Trans. Ind. Electron.*, vol. 62, no. 7, pp. 4398–4407, Jul. 2015.
- [8] P. Rawat, K. D. Singh, H. Chaouchi, and J. M. Bonnin, "Wireless sensor networks: A survey on recent developments and potential synergies," *J. Supercomput.*, vol. 68, no. 1, pp. 1–48, 2014.
- [9] J. Stankovic, "Wireless sensor networks," *Computer*, vol. 41, no. 10, pp. 92–95, Oct. 2008.
- [10] Y. Li, J. Li, A. Yang, Y. Zhang, B. Jiang, and D. Qiao, "Electromagnetic vibrational energy harvester with microfabricated springs and flexible coils," *IEEE Trans. Ind. Electron.*, vol. 68, no. 3, pp. 2684–2693, Mar. 2021.
- [11] K. Kim, S. Paul, D. Bang, and J. Chang, "Performance of permanent magnet synchronous generator for urban water pipeline energy harvester considering slotting and load effect on radial force characteristic," *IEEE Trans. Magn.*, vol. 57, no. 6, pp. 1–5, Jun. 2021.
- [12] T. Martinez, G. Pillonnet, and F. Costa, "A 15-mV inductor-less start-up converter using a piezoelectric transformer for energy harvesting applications," *IEEE Trans. Power Electron.*, vol. 33, no. 3, pp. 2241–2253, Mar. 2018.
- [13] N. M. Roscoe and M. D. Judd, "Optimization of voltage doublers for energy harvesting applications," *IEEE Sensors J.*, vol. 13, no. 12, pp. 4904–4911, Dec. 2013.
- [14] S.-W. Wang, Y.-W. Ke, P.-C. Huang, and P.-H. Hsieh, "Electromagnetic energy harvester interface design for wearable applications," *IEEE Trans. Circuits Syst. II, Exp. Briefs*, vol. 65, no. 5, pp. 667–671, May 2018.
- [15] S. Cheng, R. Sathe, R. D. Natarajan, and D. P. Arnold, "A voltage-multiplying self-powered AC/DC converter with 0.35-V minimum input voltage for energy harvesting applications," *IEEE Trans. Power Electron.*, vol. 26, no. 9, pp. 2542–2549, Sep. 2011.
- [16] J. Lee and S. W. Yoon, "Optimization of magnet and back-iron topologies in electromagnetic vibration energy harvesters," *IEEE Trans. Magn.*, vol. 51, no. 6, pp. 1–7, Jun. 2015.
- [17] M. Han, Q. Yuan, X. Sun, and H. Zhang, "Design and fabrication of integrated magnetic MEMS energy harvester for low frequency applications," *IEEE/ASME J. Microelectromech. Syst.*, vol. 23, no. 1, pp. 204–212, Jan. 2014.
- [18] O. Z. Olszewski, R. Houlihan, A. Blake, A. Mathewson, and N. Jackson, "Evaluation of vibrational PiezoMEMS harvester that scavenges energy from a magnetic field surrounding an AC current-carrying wire," *J. Microelectromech. Syst.*, vol. 26, no. 6, pp. 1298–1305, Dec. 2017.
- [19] A. Sokolov, D. Mallick, S. Roy, M. P. Kennedy, and E. Blokhina, "Modelling and verification of nonlinear electromechanical coupling in micro-scale kinetic electromagnetic energy harvesters," *IEEE Trans. Circuits Syst. I, Reg. Papers*, vol. 67, no. 2, pp. 565–577, Feb. 2020.
- [20] Q. Zhang and E. S. Kim, "Micromachined energy-harvester stack with enhanced electromagnetic induction through vertical integration of magnets," *IEEE/ASME J. Microelectromech. Syst.*, vol. 24, no. 2, pp. 384–394, Apr. 2015.
- [21] J. Iannacci, "Microsystem based energy harvesting (EH-MEMS): Powering pervasivity of the Internet of Things (IoT)—A review with focus on mechanical vibrations," *J. King Saud Univ.-Sci.*, vol. 31, no. 1, pp. 66–74, Jan. 2019.
- [22] T. Hosseinimehr and A. Tabesh, "Magnetic field energy harvesting from AC lines for powering wireless sensor nodes in smart grids," *IEEE Trans. Ind. Electron.*, vol. 63, no. 8, pp. 4947–4954, Aug. 2016.
- [23] P. L. Diez, I. Gabilondo, E. Alarcon, and F. Moll, "Mechanical energy harvesting taxonomy for industrial environments: Application to the railway industry," *IEEE Trans. Intell. Transp. Syst.*, vol. 21, no. 7, pp. 2696–2706, Jul. 2020.
- [24] A. Kumar, S. S. Balpande, and S. C. Anjankar, "Electromagnetic energy harvester for low frequency vibrations using MEMS," *Proc. Comput. Sci.*, vol. 79, pp. 785–792, Jan. 2016.
- [25] J. Moon and S. B. Leeb, "Power electronic circuits for magnetic energy harvesters," *IEEE Trans. Power Electron.*, vol. 31, no. 1, pp. 270–279, Jan. 2016.
- [26] S. Cao, S. Yang, J. Zheng, L. Zhang, and B. Wang, "An equivalent circuit model and energy extraction technique of a magnetostrictive energy harvester," *IEEE Trans. Appl. Supercond.*, vol. 26, no. 4, pp. 1–6, Jun. 2016.
- [27] S. Paul, S. Bashir, and J. Chang, "Design of a novel electromagnetic energy harvester with dual core for deicing device of transmission lines," *IEEE Trans. Magn.*, vol. 55, no. 2, pp. 1–4, Feb. 2019.
- [28] P.-C. Yeh, T.-H. Chien, M.-S. Hung, C.-P. Chen, and T.-K. Chung, "Attachable magnetic-piezoelectric energy-harvester powered wireless temperature sensor nodes for monitoring of high-power electrical facilities," *IEEE Sensors J.*, vol. 21, no. 9, pp. 11140–11154, May 2021.
- [29] D. A. Vieira, M. P. Santos, A. C. F. M. Costa, and C. P. Souza, "Ni-Zn ferrite core characterization for magnetic-based energy harvesting application," *IEEE Latin Amer. Trans.*, vol. 14, no. 9, pp. 4070–4075, Sep. 2016.
- [30] U. Ahmed, U. Aydin, L. Daniel, and P. Rasilo, "3-D magneto-mechanical finite element analysis of Galfenol-based energy harvester using an equivalent stress model," *IEEE Trans. Magn.*, vol. 57, no. 2, pp. 1–5, Feb. 2021.
- [31] S. Cao, P. Zhang, J. Zheng, Z. Zhao, and B. Wang, "Dynamic nonlinear model with eddy current effect for stress-driven Galfenol energy harvester," *IEEE Trans. Magn.*, vol. 51, no. 11, pp. 1–4, Nov. 2015.
- [32] S. Cao, J. Zheng, Y. Guo, Q. Li, J. Sang, B. Wang, and R. Yan, "Dynamic characteristics of Galfenol cantilever energy harvester," *IEEE Trans. Magn.*, vol. 51, no. 3, pp. 1–4, Mar. 2015.
- [33] Y. Yang, U. Radhakrishna, J. F. Hunter, T. W. Eagar, and J. H. Lang, "An electromagnetic translational vibration energy harvester fabricated in MP35N alloy," *J. Microelectromech. Syst.*, vol. 29, no. 6, pp. 1518–1522, Dec. 2020.
- [34] Q. Zhang and E. S. Kim, "Microfabricated electromagnetic energy harvesters with magnet and coil arrays suspended by silicon springs," *IEEE Sensors J.*, vol. 16, no. 3, pp. 634–641, Feb. 2016.
- [35] A. Ghaneizadeh, M. Joodaki, J. Borcsok, A. Golmakani, and K. Mafinezhad, "Analysis, design, and implementation of a new extremely ultrathin 2-D-isotropic flexible energy harvester using symmetric patch FSS," *IEEE Trans. Microw. Theory Techn.*, vol. 68, no. 6, pp. 2108–2115, Jun. 2020.
- [36] H. Lee, M. D. Noh, and Y.-W. Park, "Optimal design of electromagnetic energy harvester using analytic equations," *IEEE Trans. Magn.*, vol. 53, no. 11, pp. 1–5, Nov. 2017.
- [37] T. J. Kazmierski, L. Wang, B. M. Al-Hashimi, and G. V. Merrett, "An explicit linearized state-space technique for accelerated simulation of electromagnetic vibration energy harvesters," *IEEE Trans. Comput.-Aided Design Integr. Circuits Syst.*, vol. 31, no. 4, pp. 522–531, Apr. 2012.
- [38] E. Dallago, M. Marchesi, and G. Venchi, "Analytical model of a vibrating electromagnetic harvester considering nonlinear effects," *IEEE Trans. Power Electron.*, vol. 25, no. 8, pp. 1989–1997, Aug. 2010.
- [39] B. Rezaealam, T. Ueno, and S. Yamada, "Finite element analysis of Galfenol unimorph vibration energy harvester," *IEEE Trans. Magn.*, vol. 48, no. 11, pp. 3977–3980, Nov. 2012.
- [40] Y. Kuang, Z. J. Chew, T. Ruan, and M. Zhu, "Magnetic field energy harvesting from current-carrying structures: Electromagnetic-circuit coupled model, validation and application," *IEEE Access*, vol. 9, pp. 46280–46291, 2021.
- [41] L. Zhao and E. S. Kim, "Analytical dual-charged surface model for permanent magnet and its application in magnetic spring," *IEEE Trans. Magn.*, vol. 56, no. 9, pp. 1–5, Sep. 2020.
- [42] T. Sato, K. Watanabe, and H. Igarashi, "Coupled analysis of electromagnetic vibration energy harvester with nonlinear oscillation," *IEEE Trans. Magn.*, vol. 50, no. 2, pp. 313–316, Feb. 2014.
- [43] P. Li, Y. Wen, C. Jia, and X. Li, "A magnetolectric composite energy harvester and power management circuit," *IEEE Trans. Ind. Electron.*, vol. 58, no. 7, pp. 2944–2951, Sep. 2010.
- [44] J. Leicht and Y. Manoli, "A 2.6  $\mu\text{W}$  –1.2 mW autonomous electromagnetic vibration energy harvester interface IC with conduction-angle-controlled MPPT and up to 95% efficiency," *IEEE J. Solid-State Circuits*, vol. 52, no. 9, pp. 2448–2462, Sep. 2017.



- [45] B. Park, S. Huh, J. Kim, H. Kim, Y. Shin, S. Woo, J. Park, A. Brito, D. Kim, H. H. Park, O. Jeong, J.-I. Koo, and S. Ahn, "The magnetic energy harvester with improved power density using saturable magnetizing inductance model for maintenance applications near high voltage power line," *IEEE Access*, vol. 9, pp. 82661–82674, 2021.
- [46] S. Yuan, Y. Huang, J. F. Zhou, Q. Xu, C. Y. Song, and G. Yuan, "A high-efficiency helical core for magnetic field energy harvesting," *IEEE Trans. Power Electron.*, vol. 32, no. 7, pp. 5365–5376, Jul. 2017.
- [47] S. Yuan, Y. Huang, J. Zhou, Q. Xu, C. Song, and P. Thompson, "Magnetic field energy harvesting under overhead power lines," *IEEE Trans. Power Electron.*, vol. 30, no. 11, pp. 6191–6202, Nov. 2015.
- [48] J. Moon and S. B. Lee, "Analysis model for magnetic energy harvesters," *IEEE Trans. Power Electron.*, vol. 30, no. 8, pp. 4302–4311, Aug. 2015.
- [49] W. Wang, C. Xu, C. Zhang, and C. Chen, "Start-up and saturation optimization of high-power energy harvester with compound topologies overhead AC transmission line," *IEEE J. Emerg. Sel. Topics Power Electron.*, vol. 8, no. 4, pp. 3607–3617, Dec. 2020.
- [50] J. Wang and W. Chen, "Output characteristics analysis of energy harvesting current transformer," *IEEE Sensors J.*, vol. 21, no. 20, pp. 22595–22602, Oct. 2021.
- [51] Q. Tang and X. Li, "Two-stage wideband energy harvester driven by multimode coupled vibration," *IEEE/ASME Trans. Mechatronics*, vol. 20, no. 1, pp. 115–121, Feb. 2015.
- [52] T.-K. Chung, C.-M. Wang, P.-C. Yeh, T.-W. Liu, C.-Y. Tseng, and C.-C. Chen, "A three-axial frequency-tunable piezoelectric energy harvester using a magnetic-force configuration," *IEEE Sensors J.*, vol. 14, no. 9, pp. 3152–3163, Sep. 2014.
- [53] P. Deepak and B. George, "Piezoelectric energy harvesting from a magnetically coupled vibrational source," *IEEE Sensors J.*, vol. 21, no. 3, pp. 3831–3838, Feb. 2021.
- [54] A. Khaligh, P. Zeng, X. Wu, and Y. Xu, "A hybrid energy scavenging topology for human-powered mobile electronics," in *Proc. 34th Annu. Conf. IEEE Ind. Electron.*, Orlando, FL, USA, Nov. 2008, pp. 448–453.
- [55] A. Khaligh, P. Zeng, and C. Zheng, "Kinetic energy harvesting using piezoelectric and electromagnetic technologies-state of the art," *IEEE Trans. Ind. Electron.*, vol. 57, no. 3, pp. 850–860, Mar. 2010.
- [56] Y. Yang, T. Cai, S. Xue, X. Song, and X. Cui, "High performance hybrid piezoelectric-electromagnetic energy harvester for scavenging energy from low-frequency vibration excitation," *IEEE Access*, vol. 8, pp. 206503–206513, 2020.
- [57] J. Blanco, F. Bolos, A. Collado, and A. Georgiadis, "RF-energy harvesting and wireless power transfer efficiency from digitally modulated signals," in *Proc. IEEE 15th Medit. Microw. Symp. (MMS)*, Nov. 2015, pp. 1–4.
- [58] K. Pirapaharan, K. Gunawickrama, D. S. De Silva, M. S. S. R. De Silva, T. L. K. C. Dharmawardhana, W. G. D. C. Indunil, C. B. Wickramasinghe, and C. V. Aravind, "Energy harvesting through the radio frequency wireless power transfer," in *Proc. IEEE Int. RF Microw. Conf. (RFM)*, Dec. 2013, pp. 376–381.
- [59] H. Reinisch, S. Gruber, H. Unterassinger, M. Wiessflecker, G. Hofer, W. Pribyl, and G. Holweg, "An electro-magnetic energy harvesting system with 190 nW idle mode power consumption for a BAW based wireless sensor node," *IEEE J. Solid-State Circuits*, vol. 46, no. 7, pp. 1728–1741, Jul. 2011.
- [60] P. S. Yedavalli, T. Riihonen, X. Wang, and J. M. Rabaey, "Far-field RF wireless power transfer with blind adaptive beamforming for Internet of Things devices," *IEEE Access*, vol. 5, pp. 1743–1752, 2017.
- [61] G. Monti, F. Congedo, P. Arcuti, and L. Tarricone, "Resonant energy scavenger for sensor powering by spurious emissions from compact fluorescent lamps," *IEEE Sensors J.*, vol. 14, no. 7, pp. 2347–2354, Jul. 2014.
- [62] X. Tian, K. T. Chau, W. Liu, and C. H. T. Lee, "Analysis of multi-coil omnidirectional energy harvester," *IEEE Trans. Magn.*, vol. 57, no. 2, pp. 1–6, Feb. 2021.
- [63] J. Zhou, P. Zhang, J. Han, L. Li, and Y. Huang, "Metamaterials and metasurfaces for wireless power transfer and energy harvesting," *Proc. IEEE*, vol. 110, no. 1, pp. 31–55, Jan. 2022.
- [64] J. Huang, Y. Zhou, Z. Ning, and H. Gharavi, "Wireless power transfer and energy harvesting: Current status and future prospects," *IEEE Wireless Commun.*, vol. 26, no. 4, pp. 163–169, Aug. 2019.
- [65] B. Clerckx, Z. Popović, and R. Murch, "Future networks with wireless power transfer and energy harvesting," *Proc. IEEE*, vol. 110, no. 1, pp. 3–7, Jan. 2022.
- [66] C. Zhang, N. Tang, W. Zhong, C. K. Lee, and R. S. Y. Hui, "A new energy harvesting and wireless power transfer system for smart grid," in *Proc. IEEE 7th Int. Symp. Power Electron. Distrib. Gener. Syst. (PEDG)*, Jun. 2016, pp. 1–5.
- [67] G. K. Ijamaru, K. L. M. Ang, and J. K. P. Seng, "Wireless power transfer and energy harvesting in distributed sensor networks: Survey, opportunities, and challenges," *Int. J. Distrib. Sensor Netw.*, vol. 18, no. 3, pp. 1–23, 2022.
- [68] W. Nan, H. Yuncheng, and F. Jiyang, "Bistable energy harvester using easy snap-through performance to increase output power," *Energy*, vol. 226, pp. 1–8, Jul. 2021.
- [69] K. A. Singh, R. Kumar, and R. J. Weber, "A broadband bistable piezoelectric energy harvester with nonlinear high-power extraction," *IEEE Trans. Power Electron.*, vol. 30, no. 12, pp. 6763–6774, Dec. 2015.
- [70] S. P. Pellegrini, N. Tolou, M. Schenk, and J. L. Herder, "Bistable vibration energy harvesters: A review," *J. Intell. Mater. Syst. Struct.*, vol. 24, no. 11, pp. 1303–1312, 2012.
- [71] P. Podder, A. Amann, and S. Roy, "Combined effect of bistability and mechanical impact on the performance of a nonlinear electromagnetic vibration energy harvester," *IEEE/ASME Trans. Mechatronics*, vol. 21, no. 2, pp. 727–739, Apr. 2016.
- [72] K. A. Singh, M. Pathak, R. J. Weber, and R. Kumar, "A self-propelled mechanism to increase range of bistable operation of a piezoelectric cantilever-based vibration energy harvester," *IEEE Trans. Ultrason., Ferroelectr., Freq. Control*, vol. 65, no. 11, pp. 2184–2194, Nov. 2018.
- [73] H. Deng, Z. Wang, Y. Du, J. Zhang, M. Ma, and X. Zhong, "A compact and flexible nonbeam-type vibrational energy harvesting device with bistable characteristics," *IEEE/ASME Trans. Mechatronics*, vol. 24, no. 1, pp. 282–292, Feb. 2019.
- [74] J. Wiegand, "Bistable magnetic device," U.S. Patent 3 820 090 A, 1974.
- [75] S. Saggini, F. Ongaro, L. Corradini, and A. Affanni, "Low-power energy harvesting solutions for Wiegand transducers," *IEEE J. Emerg. Sel. Topics Power Electron.*, vol. 3, no. 3, pp. 766–779, Sep. 2015.
- [76] J. Chotai, M. Thakker, and Y. Takemura, "Single-bit, self-powered digital counter using a Wiegand sensor for rotary applications," *Sensors*, vol. 20, no. 14, pp. 1–10, 2020.
- [77] C.-C. Chang and J.-Y. Chang, "Novel Wiegand-effect based energy harvesting device for linear magnetic positioning system," *Microsyst. Technol.*, vol. 26, no. 11, pp. 3421–3426, Nov. 2020.
- [78] Y. H. Chen, C. Lee, Y. J. Wang, Y. Y. Chang, and Y. C. Chen, "Energy harvester based on an eccentric pendulum and Wiegand wires," *Micromachines*, vol. 13, no. 4, pp. 1–16, 2022.
- [79] W. He, P. Li, Y. Wen, J. Zhang, A. Yang, and C. Lu, "Energy harvesting from two-wire power cords using magnetoelectric transduction," *IEEE Trans. Magn.*, vol. 50, no. 8, pp. 1–5, Aug. 2014.
- [80] Q. Zhang, Y. Wang, and E. S. Kim, "Electromagnetic energy harvester with flexible coils and magnetic spring for 1–10 Hz resonance," *J. Microelectromech. Syst.*, vol. 24, no. 4, pp. 1193–1206, Aug. 2015.
- [81] Y. Liu, W. Fu, W. Li, and M. Sun, "Design and analysis of a shoe-embedded power harvester based on magnetic gear," *IEEE Trans. Magn.*, vol. 52, no. 7, pp. 1–4, Jul. 2016.
- [82] L. Xie and M. Cai, "An in-shoe harvester with motion magnification for scavenging energy from human foot strike," *IEEE/ASME Trans. Mechatronics*, vol. 20, no. 6, pp. 3264–3268, Dec. 2015.
- [83] Ö. Zorlu, E. T. Topal, and H. Külah, "A vibration-based electromagnetic energy harvester using mechanical frequency up-conversion method," *IEEE Sensors J.*, vol. 11, no. 2, pp. 481–488, Feb. 2011.
- [84] T. Galchev, H. Kim, and K. Najafi, "Micro power generator for harvesting low-frequency and nonperiodic vibrations," *J. Microelectromech. Syst.*, vol. 20, no. 4, pp. 852–866, 2011.
- [85] M. Beyaz, S. Habibiabad, H. Yıldız, U. Göreke, and K. Azgın, "A compact energy transducer for power generation from respiration," *J. Microelectromech. Syst.*, vol. 28, no. 3, pp. 504–512, Jun. 2019.
- [86] F. A. Samad, M. F. Karim, V. Paulose, and L. C. Ong, "A curved electromagnetic energy harvesting system for wearable electronics," *IEEE Sensors J.*, vol. 16, no. 7, pp. 1969–1974, Apr. 2016.
- [87] K. El-Rayes, S. Gabran, E. Abdel-Rahman, and W. Melek, "Variable-flux biaxial vibration energy harvester," *IEEE Sensors J.*, vol. 18, no. 8, pp. 3218–3227, Apr. 2018.
- [88] H. Zhang, "Power generation transducer from magnetostrictive materials," *Appl. Phys. Lett.*, vol. 98, no. 23, pp. 1–3, 2011.
- [89] G. Backman, B. Lawton, and N. A. Morley, "Magnetostrictive energy harvesting: Materials and design study," *IEEE Trans. Magn.*, vol. 55, no. 7, pp. 1–6, Jul. 2019.

- [90] C. S. Clemente, D. Davino, and V. P. Loschiavo, "Analysis of a magnetostrictive harvester with a fully coupled nonlinear FEM modeling," *IEEE Trans. Magn.*, vol. 57, no. 6, pp. 1–4, Jun. 2021.
- [91] M. Zucca, O. Bottauscio, C. Beatrice, A. Hadadian, F. Fiorillo, and L. Martino, "A study on energy harvesting by amorphous strips," *IEEE Trans. Magn.*, vol. 50, no. 11, pp. 1–4, Nov. 2014.
- [92] M. Zucca, O. Bottauscio, C. Beatrice, and F. Fiorillo, "Modeling amorphous ribbons in energy harvesting applications," *IEEE Trans. Magn.*, vol. 47, no. 10, pp. 4421–4424, Oct. 2011.
- [93] K. Kecik, A. Mitura, S. Lenci, and J. Warminski, "Energy harvesting from a magnetic levitation system," *Int. J. Non-Linear Mech.*, vol. 94, pp. 200–206, Sep. 2017.
- [94] Z. Zhang, J. Kan, S. Wang, H. Wang, C. Yang, and S. Chen, "Performance dependence on initial free-end levitation of a magnetically levitated piezoelectric vibration energy harvester with a composite cantilever beam," *IEEE Access*, vol. 5, pp. 27563–27572, 2017.
- [95] M. Gao, P. Wang, Y. Cao, R. Chen, and D. Cai, "Design and verification of a rail-borne energy harvester for powering wireless sensor networks in the railway industry," *IEEE Trans. Intell. Transp. Syst.*, vol. 18, no. 6, pp. 1596–1609, Jun. 2017.
- [96] M. Gao, P. Wang, Y. Wang, and L. Yao, "Self-powered ZigBee wireless sensor nodes for railway condition monitoring," *IEEE Trans. Intell. Transp. Syst.*, vol. 19, no. 3, pp. 900–909, Mar. 2018.
- [97] P. Carneiro, M. P. S. D. Santos, A. Rodrigues, J. A. F. Ferreira, J. A. O. Simões, A. T. Marques, and A. L. Kholkin, "Electromagnetic energy harvesting using magnetic levitation architectures: A review," *Appl. Energy*, vol. 260, pp. 1–22, Feb. 2020.
- [98] W. He, J. Zhang, S. Yuan, A. Yang, and C. Qu, "A three-dimensional magneto-electric vibration energy harvester based on magnetic levitation," *IEEE Magn. Lett.*, vol. 8, pp. 1–3, 2017.
- [99] Y. Zhu and J. W. Zu, "A magnetoelectric generator for energy harvesting from the vibration of magnetic levitation," *IEEE Trans. Magn.*, vol. 48, no. 11, pp. 3344–3347, Nov. 2012.
- [100] R. Liu, Z. Xu, Y. Jin, and W. Wang, "Design and research on a nonlinear 2DOF electromagnetic energy harvester with velocity amplification," *IEEE Access*, vol. 8, pp. 159947–159955, 2020.
- [101] V. Nico, R. Frizzell, and J. Punch, "The identification of period doubling in a nonlinear two-degree-of-freedom electromagnetic vibrational energy harvester," *IEEE/ASME Trans. Mechatronics*, vol. 25, no. 6, pp. 2973–2980, Dec. 2020.
- [102] S. Li, Y. Wang, M. Yang, Y. Sun, F. Wu, J. Dai, P. Wang, and M. Gao, "Investigation on a broadband magnetic levitation energy harvester for railway scenarios," *J. Intell. Mater. Syst. Struct.*, vol. 33, no. 5, pp. 653–668, Mar. 2022.
- [103] S. Ahmim, M. Almanza, V. Loyau, A. Pasko, F. Mazaleyrat, and M. LoBue, "A thermal energy harvester using LaFeSi magnetocaloric materials," *IEEE Trans. Magn.*, vol. 57, no. 2, pp. 1–5, Feb. 2021.
- [104] S. Ahmim, M. Almanza, V. Loyau, F. Mazaleyrat, A. Pasko, F. Parrain, and M. LoBue, "Self-oscillation and heat management in a LaFeSi based thermomagnetic generator," *J. Magn. Magn. Mater.*, vol. 540, pp. 1–9, Dec. 2021.
- [105] D. N. Ba, L. Becerra, N. Casaretto, J.-E. Duvauchelle, M. Marangolo, S. Ahmim, M. Almanza, and M. LoBue, "Magnetocaloric Gadolinium thick films for energy harvesting applications," *AIP Adv.*, vol. 10, no. 3, pp. 1–4, 2020.
- [106] M. Ujihara, G. P. Carman, and D. G. Lee, "Thermal energy harvesting device using ferromagnetic materials," *Appl. Phys. Lett.*, vol. 91, no. 9, Aug. 2007, Art. no. 093508.
- [107] M. A. Hamad, H. R. Alamri, and M. E. Harb, "Environmentally friendly energy harvesting using magnetocaloric solid-state nanoparticles as magnetic refrigerator," *J. Low Temp. Phys.*, vol. 204, nos. 1–2, pp. 57–63, Jul. 2021.
- [108] Y. Xu, S. Bader, and B. Oelmann, "A survey on variable reluctance energy harvesters in low-speed rotating applications," *IEEE Sensors J.*, vol. 18, no. 8, pp. 3426–3435, Apr. 2018.
- [109] M. Kroener, N. Moll, S. K. T. Ravindran, P. Mehne, and P. Woias, "Characterization of a variable reluctance harvester," *J. Phys., Conf. Ser.*, vol. 557, no. 1, Nov. 2014, Art. no. 012035.
- [110] Y. Gong, S. Wang, Z. Xie, T. Zhang, W. Chen, X. Lu, Q. Zeng, Y. Gao, and W. Huang, "Self-powered wireless sensor node for smart railway axle box bearing via a variable reluctance energy harvesting system," *IEEE Trans. Instrum. Meas.*, vol. 70, pp. 1–11, 2021.
- [111] Y. Xu, Y. Zhang, S. Bader, B. Oelmann, and J. Cao, "Three-phase variable reluctance energy harvesting," *Energy Convers. Manage.*, X, vol. 14, pp. 1–13, May 2022.
- [112] Y. Xu, S. Bader, and B. Oelmann, "Design, modeling and optimization of an m-shaped variable reluctance energy harvester for rotating applications," *Energy Convers. Manage.*, vol. 195, pp. 1280–1294, Sep. 2019.
- [113] A. Bibo, R. Masana, A. King, G. Li, and M. F. Daqaq, "Electromagnetic ferrofluid-based energy harvester," *Phys. Lett. A.*, vol. 376, no. 32, pp. 2163–2166, Jun. 2012.
- [114] Q. Liu, S. F. Alazemi, M. F. Daqaq, and G. Li, "A ferrofluid based energy harvester: Computational modeling, analysis, and experimental validation," *J. Magn. Magn. Mater.*, vol. 449, pp. 105–118, Mar. 2018.
- [115] S. Wu, P. C. K. Luk, C. Li, X. Zhao, and Z. Jiao, "Investigation of an electromagnetic wearable resonance kinetic energy harvester with ferrofluid," *IEEE Trans. Magn.*, vol. 53, no. 9, pp. 1–7, Sep. 2017.
- [116] S. Wang, Y. Liuy, D. Liz, and H. Wangx, "An electromagnetic energy harvester using ferrofluid as a lubricant," *Mod. Phys. Lett. B.*, vol. 32, no. 34, pp. 1–6, 2018.
- [117] Q. Liu, M. F. Daqaq, and G. Li, "Performance analysis of a ferrofluid-based electromagnetic energy harvester," *IEEE Trans. Magn.*, vol. 54, no. 5, pp. 1–14, May 2018.
- [118] Y. Wang, Q. Zhang, L. Zhao, and E. S. Kim, "Non-resonant electromagnetic broad-band vibration-energy harvester based on self-assembled ferrofluid liquid bearing," *J. Microelectromech. Syst.*, vol. 26, no. 4, pp. 809–819, 2017.
- [119] L. Buccolini and M. Conti, "An energy harvester interface for self-powered wireless speed sensor," *IEEE Sensors J.*, vol. 17, no. 4, pp. 1097–1104, Feb. 2017.



**JAVAD ENAYATI** was born in Shahi, Iran, in 1986. He received the B.S. degree in power electrical engineering from the Nooshirvani University of technology, Iran, in 2009, and the M.S. degree in power electrical engineering and the Ph.D. degree from the University of Semnan, in 2012 and 2017, respectively. He is currently a Postdoctoral Researcher of automotive engineering specialising in automotive electrical and electromechanical systems with the Department of Engineering and Technology, University of Hertfordshire. He is an Electrical Consultant with the Research and Development Department, Mazinoor Lighting Industries, Babol. His research interests include lighting, state estimation, system identification, automotive systems reliability, and system engineering.



**PEDRAM ASEF** (Senior Member, IEEE) received the Ph.D. degree (*cum laude*) in electrical engineering from Universitat Politècnica de Catalunya (UPC), Barcelona, Spain, in 2018. He is a Senior Lecturer with the Department of Engineering and Technology, University of Hertfordshire where he is leading the Electrification and Intelligent Mobility Research Laboratory. He has been the Lead Representative of the IEEE Power and Energy Society, Young Professionals, in Europe region, since 2018. His projects are funded by the European Space Agency (ESA), UKRI, European Commission, and Texas State Center for Port Management. His research interests include electrical machinery and drives, intelligent energy systems, and machine learning. His Editorial activities are limited to IET Generation, Transmission Distribution, Wiley, Sustainability, and Distributed Generation Alternative Energy Journals. In 2019, he was appointed as the Star Reviewer of IEEE TRANSACTIONS ON ENERGY CONVERSION.